Improving Anodes for Lithium Ion Batteries

GERARD K. SIMON and TARUN GOSWAMI

As energy demands increase for applications such as automotive, military, aerospace, and biomedical, lithium-ion battery capacities are forced to increase in a corresponding manner. For this reason, much research is directed toward the development of improved battery anodes. Carbon nanotubes (CNTs), silicon, tin, and nanocomposites with these metals are the leading candidates for the next generation of lithium-ion battery anodes, leading to capacities 3 to 10 times that of graphite alone. This review looks at some of the studies addressing high capacity lithium-ion battery anodes.

© The Minerals, Metals & Materials Society and ASM International 2010

I. INTRODUCTION

LITHIUM-ION technology has revolutionized the battery industry and made numerous miniaturized electronic devices possible. The success of hybrid and electric vehicles in development also depends on the Li-ion battery. The low weight and high capacity of this battery chemistry are key enablers to longer range and lower operating costs in the auto industry as well as the aerospace industry. In the biomedical industry, these same features will contribute significantly to the quality of life of prosthetic wearers and users of cochlear implants and spinal cord stimulators. They will also enable the implementation of ground-breaking devices such as rechargeable pacemakers.

In the interest of increasing the capacity of lithium-ion batteries, the anode is being heavily researched. It is graphite based in current batteries and intercalates lithium well with a theoretical specific capacity of 372 mAh/g. It is also inexpensive and widely available. This limit on the specific capacity is partially imposed by the thermodynamic equilibrium saturation composition of LiC_6.[1,2] In practice, one can expect to attain a reversible capacity in the vicinity of 350 mAh/g.[3–5] However, research efforts have demonstrated that anode capacity boosts of 3 to 10 times what is currently available will be possible in the near future.

II. NANOSIZED CARBON BASED ANODE MATERIALS

Carbon nanotubes (CNTs) are a large part of the anode material research. While CNTs are materials of interest to unlock new capabilities in a variety of fields,

in battery technology, they are mostly being developed to increase the specific capacity of anodes. CNTs produce very interesting results.

Raw unprepared multiwalled carbon nanotubes (MWNTs) have shown a fairly low reversible capacity (C_{rev}) ranging from as low as 175 to 237 mAh/g[6,7] at a rate of 30 mA/g. These are CNTs with diameters between 4 and 50 nm and lengths of several microns. They are also often capped, possibly limiting their intercalation abilities. Once the caps of MWNTs are removed by oxidation treatment in air, the C_{rev} improves to 625 mAh/g.[7] This is attributed to lithium intercalation directly into the CNT cores.[4,8]

As grown, single wall carbon nanotubes (SWNTs) have achieved a C_{rev} of 450 mAh/g, exceeding the capacity of graphite.[1] Purification of the nanotubes is a simple and effective step to remove nonactive materials and improve the total specific capacity of the material. After purification to 80 pct purity by filtering the materials through a micropore membrane, the SWNTs' C_{rev} increased to 600 mAh/g after the first cycle, while the irreversible capacity (C_{irr}) was 1600 mAh/g. Finally, a 1000 mAh/g C_{rev} was achieved on the first cycle by ball milling the SWNTs.[8] In this example, the C_{irr} was 700 mAh/g (1700 mAh/g total capacity). After the second cycle, the total capacity dropped to 1000 mAh/g for a 700 mAh/g loss of capacity. Ball milling the SWNTs breaks the tubes and exposes the edges of the graphene layers to which lithium can intercalate itself. Ball milling also increases the surface area of the CNTs, allowing more lithium to intercalate. Unfortunately, the lithium is not easily deintercalated and the C_{irr} increases. These SWNTs were produced by pulsed laser ablation of a graphite target.[8,9] Swagelok-type cells,[10] without polymer binders or carbon black, were used with Li foil and nanotube films for electrodes. The cells were charged and discharged at a rate of 50 mA/g.

Another method of pushing the capacity of CNTs beyond that of the raw product is by acid etching. Acid etching has the effect of shortening the MWNTs and creating defects in the MWNT surface. This increases the surface area of the CNTs and creates additional

GERARD K. SIMON, Postdoctoral Candidate, and TARUN GOSWAMI, Joint Associate Professor of Biomedical/Orthopaedics, are with the Department of Biomedical, Industrial and Human Factors Engineering, Wright State University, Dayton OH, 45435. Contact e-mail: kenpo-g@sbcglobal.net

intercalation sites. After purifying and etching, MWNTs achieved a C_{rev} of 597 mAh/g for a 20 hour etch and 681 mAh/g for a 10 hour etch.[11] Unfortunately, these results come with high irreversible capacities (1229 mAh/g for a 20 hour etch). The electrochemical tests were performed at a rate of 50 mA/g. These MWNTs were made by a thermal chemical vapor deposition (CVD) method,[11–13] purified to 95 pct purity in HF acid and distilled water for 18 hours, and gas phase oxidized in a 15 pct air/Ar mixture at 550 °C for 1 hour. After sonication in concentrated HCl acid (37 pct) for 10 minutes, the MWNTs were filtered and dried. Acid etching was accomplished in a 3:1 ratio of concentrated H_2SO_4 acid (96 pct) and HNO_3 acid (70 pct) for 5 to 20 hours.[11] While one may expect to increase the C_{rev} by creating more defects, the opposite may also be true. In the work discussed here, the 10 hour etch CNTs actually had a better capacity than the 20 hour etch CNTs. The irreversible capacity (C_{irr}) was also higher for the 20 hour etch, indicating that lithium is not easily removed from the artificially created intercalation sites. Therefore, defect creation increased the total capacity at the expense of C_{rev}.

The CVD MWNTs were 10 to 20 nm in diameter and over 10 μm in length, and the AE MWNTs were 2 to 20 nm in diameter and over 1 μm in length with closed ends. Chemically etching and sonicating the CVD MWNTs reduced the MWNT lengths to 0.2 to 2 μm with the ends opened.[11] While no charge or discharge rate was given for this work, we can still see that etching the MWNTs can create defects in the MWNT sides (additional intercalation sites for lithium), increasing the capacity. This correlates with assertions that lateral defects in the MWNTs allow for lithium intercalation, possibly by creating fractures in the graphite layers.[14,15] However, the creation of locations in the CNT structure for intercalation also brings the risk of significantly increasing the irreversible capacity.

Buckypapers, on the other hand, use as-grown purified or unpurified nanotubes and are more focused on developing an easy to fabricate, lower cost (than processed CNTs), but high performing anode. The nanotubes are normally dispersed by ultrasonication and vacuum filtered through membranes of polyvinylidene fluoride, cellulose, poly(tetrafluoroethylene), or similar materials to form a self-standing mat that is dried for 12 to 24 hours. Several solvents may be used for dispersal and they include Triton X-100 (Union Carbide, Somerset, NJ), acetone, water, and n-methylpyrrolidone, among others. Buckypapers may also be made directly from reflux solutions following acid reflux purification.[16] After several cycles, the reversible capacity of SWNT papers was found to range from 175 mAh/g for 95 pct pure SWNTs tested with an ethylene carbonate (EC):dimethyl carbonate (DMC) electrolyte[16,17] to 520 mAh/g for high purity SWNT papers tested with an EC:propylene carbonate (PC):DMC electrolyte.[16] While the use of PC in the electrolyte may lead to increased capacity, it is known to cause exfoliation of graphene layers in graphitic carbons.[18,19] Multiwalled carbon nanotube buckypapers were found to have a reversible capacity range from 150

to 225 mAh/g after 20 cycles at a C/5 rate.[20] Again, the performance depended upon the electrolyte being used with the EC:PC:diethyl carbonate electrolyte providing the best performance. The performance of the buckypaper anodes was not sufficient for them to become a serious competitor to graphite. While the use of CNTs greatly increases the surface area of the anode, the SEI formation is also increased and this results in the trapping of more lithium ions and higher irreversible losses. The irreversible losses of the SWNT papers were as high as 400 mAh/g, while the MWNT papers' losses were as high as 340 mAh/g.[16,20] Compare these values to graphite's C_{irr} of 22 mAh/g.[3–5]

Graphene sheets, two-dimensional layers of carbon atoms, are also being studied as potential anode components for lithium-ion batteries. While the graphene sheets are normally stacked in numerous layers when found in graphite form, they appear to offer greater performance when used in very few layers. Four layers of graphene sheets, approximately 2.1-nm thick, were prepared by oxidation and rapid thermal expansion of graphite powder. After 40 cycles, this material was still capable of producing a C_{rev} of 848 mAh/g at a rate of 100 mA/g.[21] This compares well to the results obtained from graphene sheets that were produced by exfoliation of graphite crystals, and were 6 to 16 layers thick. These sheets were only able to produce a 240 mAh/g C_{rev} also at a rate of 100 mA/g.[22] With these results, we may assume that minimizing the number of layers in graphene sheets may be beneficial to anode performance in lithium-ion batteries. The loss of efficiency with increasing number of layers may be a result of the formation of the SEI, which increases with more layers, and the trapping of lithium ions, which also increases.

III. NANOWIRES

Nanowires of silicon, germanium, and tin-oxide are interesting candidates for Li-ion battery anodes because of their ability to alloy with large amounts of lithium. Their theoretical capacities are among the largest at 4200 mAh/g for silicon,[23] 1625 mAh/g for germanium,[24,25] and 1491 mAh/g for tin-oxide (SnO_2).[26] Problems arise when these materials are used in their bulk forms. They experience large changes in volume during lithium insertion and deinsertion,[24,27] 400 pct for silicon and 370 pct for germanium, for example. The large volume changes lead to pulverization, capacity fade,[23,28] and loss of electrical contact in the electrodes.[23,29] The use of nanowires allows the materials to undergo facile strain relaxation, expanding freely radially and axially, consistent with prior work, which indicated that particles small in size (micro- or nanoscale) will not fracture any further.[23,30,31]

Silicon nanowires grown directly onto stainless steel substrates (Figure 1), using the vapor-liquid-solid template-free growth method,[32–35] were capable of a 3193 mAh/g C_{rev} (C_{irr} of 1084 mAh/g) over 10 cycles.[23] This occurred with a C/20 rate, and there is some reduction in capacity with increased rates. At the 1 C rate, the C_{rev} drops to 2100 mAh/g (C_{irr} of 2177 mAh/g).
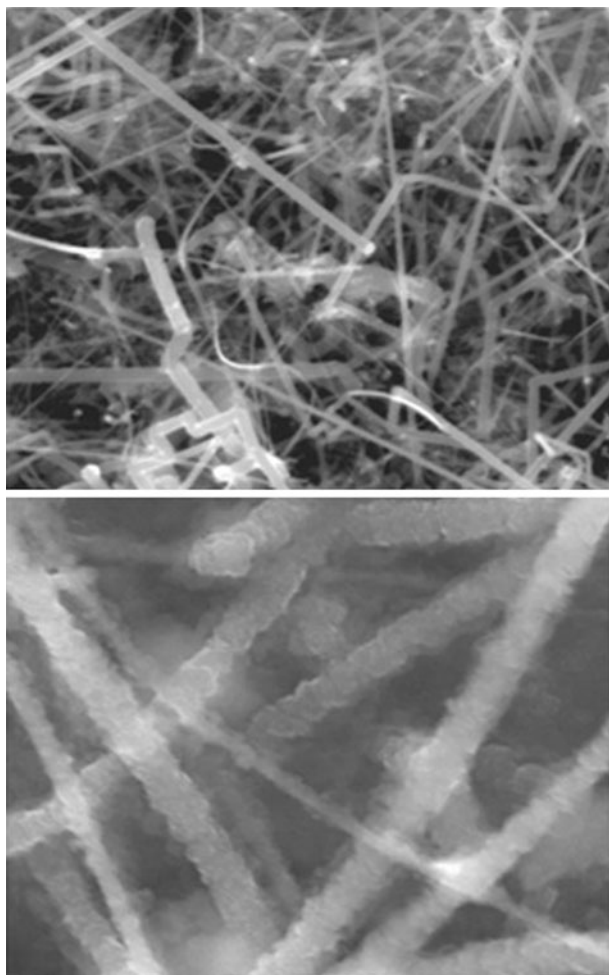
Fig. 1—Silicon nanowires before lithiation (top) and after lithiation (bottom).[23] Scales of two scanning electron micrographs (SEMs) are identical.

This still far exceeds graphite's reversible capacity. The average diameter of these nanowires increased from 89 to 141 nm after lithiation. While the nanowires shrink in size when delithiating, they do not normally return to their condition. One can infer that there must be some detachment of the nanowires from the substrate, since it is well known that degraded electrical contact between the silicon and the rest of the anode is a large contributor to capacity loss. For improved performance, a two-phase nanowire was proposed to reduce the C_{irr} of nanowires.

A silicon nanowire anode material with a crystalline core and an amorphous shell was developed and grown by CVD to exploit the superior cycling performance of amorphous silicon with respect to crystalline silicon.[36] Amorphous silicon also pulverizes less than crystalline silicon. The crystalline silicon core directly addresses the detachment issue by forming a strong mechanical support and electron transportation path for the nanowires. The shortcoming of this type of nanowire is that it requires the cutoff voltage to remain above 150 mV to prevent the entire nanowire from interacting with lithium and undergoing a crystalline to amorphous transformation in the core. This would lead to fatigue,

large capacity fade, and risk breakage of the nanowires from the substrate. With a 0.2 C current density and a 150 mV cutoff, a 960 mAh/g C_{rev} was possible after 100 cycles with 85 pct capacity retention. Most of the loss occurred on the first cycle when the efficiency was 80.4 pct. If the cutoff was changed to 10 mV, the C_{rev} increased to 2000 mAh/g after 30 cycles, but the efficiency was only 79 pct. Since there is still some loss of capacity, breakage of the nanowires may still be playing a part in the anode performance. Regardless of the method by which the silicon is attached to the substrate, it is reasonable to expect some detachment. The substrate must be fabricated from an electrochemically inert material. Therefore, it will not expand as the nanowires do when they alloy with lithium. This leads to a stress buildup at the nanowires' base that will eventually cause cracks and detachment.

Germanium nanowires grown by the same vapor-liquid-solid method as the silicon nanowires[24,37] produced a first cycle C_{rev} of 1141 mAh/g and a C_{irr} of 1826 mAh/g. Over the next 19 cycles, the discharge capacity remains stable at approximately 1000 mAh/g when tested with a C/20 rate. When the rate is increased to 2 C, the capacity drops to 600 mA/g. These nanowires are 50 to 100 nm in diameter, 20- to 50-μm long, and, like the silicon nanowires, do not pulverize. Also, like silicon nanowires, the germanium nanowires do not retain their original shape when cycled. There is a considerable capacity loss, which, again like silicon, may be attributed to breakage of the nanotubes and failure of lithium to dealloy with the germanium. Despite its lower intercalation, germanium has a potential advantage over silicon in that the room temperature diffusivity of lithium in Ge is 400 times higher than that in silicon, possibly making it a better material for high power rate applications.[24] While germanium does not expand as much as silicon when alloying with lithium, there will still be stresses at the nanowires' base. As with the silicon nanowires, the concentrated stress leads to cracking and detachment of the germanium nanowires.

In a novel application of SnO_2 for anodes, nanowires were grown on stainless steel by the thermal evaporation technique and vapor-phase transport synthetic method.[38] These nanowires were electrochemically tested over a 0.00 to 1.2 V range at multiple rates to determine their performance. At 1 C, the total capacity of the SnO_2 was 2140 mAh/g after the first cycle, but the C_{rev} was 800 mAh/g. After 50 cycles, the C_{rev} dropped to 510 mAh/g. As the charge/discharge rate was increased, there was a corresponding decrease in the specific capacity. For example, at 3 C, the C_{rev} falls to 530 mAh/g after 20 cycles. At 10 C, the C_{rev} was 440 mAh/g after 40 cycles.

The volume expansion of tin-oxide as it alloys with lithium is less than both silicon and germanium, but still 300 pct.[38] In bulk form, it naturally leads to pulverization of the material and drives the investigation of alternate methods of using tin-oxide, such as nanowires. However, like the silicon and germanium nanowires, the substrate must be an inert, conductive material such as stainless steel or copper. If the substrate does not expand as the tin-oxide does when it alloys with lithium,

there will be stresses at the base of the nanowires that will eventually lead to breakage.

Still, it was demonstrated that both carbons and metalloids have attractive properties for anodes. Therefore, the logical extension of anode material development is the study of composite materials that will hopefully exhibit the best qualities of the carbons and metalloids.

IV. NANOCOMPOSITES

To combine the best qualities of carbon and silicon, some researchers have examined the feasibility of silicon/carbon (Si/C) composites as anode materials. These materials were prepared by decomposition of organic precursors, using high-energy mechanical milling, or a combination of both.[39]

Nanocomposites were fabricated with pyrolyzed, mechanically milled silicon and polystyrene resin or by moderate ball milling of carbon (graphite, disordered carbon, meso carbon microbeads, *etc.*) and nanocrystalline silicon. The silicon nanoparticles alloy with lithium without pulverizing, while the polystyrene resin forms a matrix that accommodates the silicon's expansion. Most of the capacity loss occurs when the silicon dealloys from the lithium and shrinks. As it shrinks, there is a loss of electrical contact with the matrix around it. Therefore, it is necessary for the matrix to have a high mechanical strength to withstand the volume change of the silicon[29] or be elastic enough to shrink when the silicon shrinks.

At a rate of 100 μA/cm^2, the pyrolyzed silicon and polystyrene resin nanocomposite has a C_{rev} of 850 mAh/g with a 1.1 pct loss of capacity each cycle.[40] The primary cause of capacity loss was from the inability of the matrix to resist the expansion of the silicon. This caused a loss of electrical contact between the silicon nanoparticles and the matrix as the silicon dealloyed from the lithium and shrank.

The ball-milled carbon and nanocrystalline silicon achieved a first cycle total capacity of 800 to 1400 mAh/g, but with poor capacity retention.[41–43] The poor capacity retention of Si/C nanocomposites may arise from incomplete dispersal of silicon throughout the carbon matrix, and longer milling times may be needed to create better adhesion between the silicon and carbon.[41] However, there is a limit to how much milling is allowable. Excessive milling approaching or exceeding 5 hours causes the formation of silicon-carbide (SiC).[44,45] As the milling time increases, the weight fraction of SiC increases while the weight fraction of silicon decreases, and after 15 hours, the silicon phase is almost completely consumed.[46] This SiC phase is electrochemically inactive and does not contribute to the capacity of the anode.[39,40]

To prevent the formation of SiC and reduce the amorphization of graphite, which also takes place in long milling operations, polyacrylonitrile was used as a diffusion barrier and o-cresol novolac epoxy resin was used to bypass SiC formation during the 15 hour milling operations.[39,46] These nanocomposites (Figure 2)
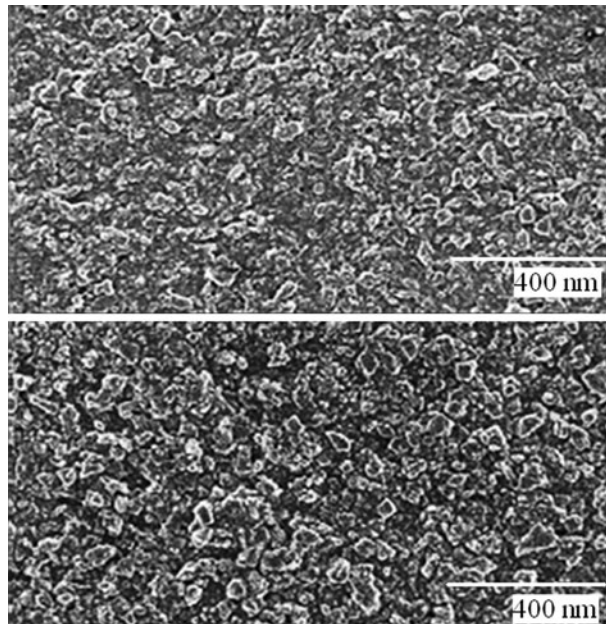

Fig. 2—SEM images of a Si/C ball-milled nanocomposite before (top) and after (bottom) 30 cycles.[46]

demonstrated reversible capacities of 660 and 640 mAh/g, respectively, at 160 mA/g, and there is almost no capacity fade after 25 to 30 cycles.

Looking at the electrochemical performance of ball-milled Si/C nanocomposites, it was demonstrated that the silicon nanoparticle size is very important to anode efficiency.[47] The nanocomposites in question were made with ball-milled silicon particles (less than 1 μm in size) and nanosized silicon powder (30 to 50 nm), each blended with graphite and pitch to form anodes. The expected outcome was that higher percentages of silicon led to higher reversible capacities and higher first cycle capacities. However, they also generated higher irreversible capacities and lower first cycle efficiencies. Most importantly, the nanosized particles performed better than the near-micron-sized particles with a 27 pct higher first cycle capacity and 7 pct higher first cycle efficiency. This clearly indicates the utility of nanosized particles in Si/C anodes.

A method to incorporate silicon nanoparticles into a nanocomposite is to encapsulate the silicon with a layer of carbon (Figure 3).[48] This was accomplished by first treating the silicon with silylating reagent to render them hydrophobic, allowing the silicon nanoparticles to be covered with a resorcinol-formaldehyde microemulsion. Carbonization of the nanoparticles was the final step. When electrochemical testing was performed, there was irreversible capacity loss on each cycle. On the first cycle at a 50 mA/g rate, the total capacity was 1730 mAh/g while the C_{rev} was 930 mAh/g. Three causes for the capacity loss were proposed: solid electrolyte interphase (SEI) formation on the carbon surface, Li$^+$ trapping in voids or cavities in the carbon, and Li$^+$ trapping in the silicon matrix. Another mechanism for capacity loss is that as the silicon nanoparticles dealloy from the lithium, they shrink
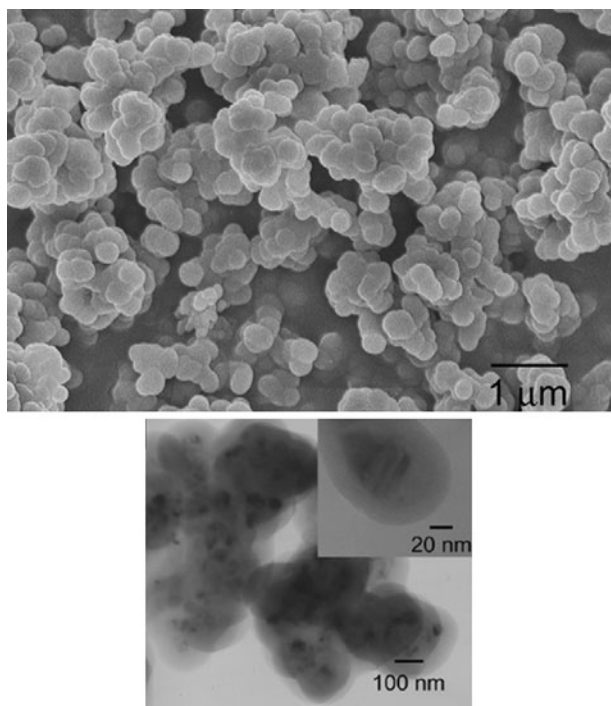
Fig. 3—SEM (top) and transmission electron micrograph of carbon-coated silicon nanoparticles prepared *via* an R-F microemulsion.[48]

Fig. 4—SEM image of SnO$_2$ nanoparticles deposited onto CNTs.[49]

within the carbon coatings (which expanded when the silicon expanded with lithium). The silicon nanoparticles inevitably begin to lose electrical contact with the carbon.

Another material that is frequently considered for a nanocomposite is tin. Tin has a fairly high theoretical specific capacity (981 mAh/g for Sn and 1491 mAh/g for SnO$_2$).[26] Like silicon, tin has a low reduction potential *vs* CNTs (+0.5 V for CNT, –0.09V for SnO$_2$, and +0.15V for Sn^{4+}). Therefore, electrodeposition of these metals onto CNTs is problematic. However, methods were developed for attaching tin nanoparticles onto CNTs with functional groups.[26,49] This has not yet been accomplished for silicon. Tin has also been combined with antimony for coating carbonaceous materials in anodes.

A tin-antimony (SnSb) alloy, which was deposited on the surface of mesophase carbon microbeads (MCMB) by coprecipitation in glycerin solution,[50] rendered performance that varied with the amount of SnSb coating the MCMBs. The best performance was obtained when a 30 wt pct percentage of SnSb was used. This formulation yielded its highest capacity after 25 cycles (380 mAh/g) and the lowest overall C$_{irr}$ (110 mAh/g). While higher concentrations of SnSb initially surrendered higher capacities, their performance quickly dropped off because they were more susceptible to agglomeration of the nanoparticles. When nanoparticles such as SnSb or silicon are smaller than 100 nm, they aggregate more aggressively as lithium is inserted and extracted.[50,51] With lower concentration of SnSb, the agglomeration is more likely to occur at sites where
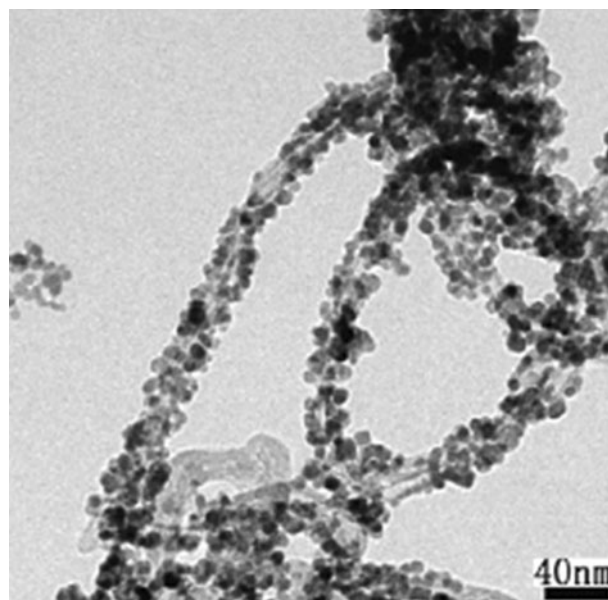
MCMBs meet, bringing the SnSb nanoparticles into close proximity with each other. If the nanoparticles are bound into place, higher concentrations may be used without risk of agglomeration.

Acidic solutions may be used to functionalize CNTs and attach SnO$_2$ nanoparticles to them (Figure 4),[49] but results in an anode with high fade and irreversible capacity after 20 cycles. The second cycle C$_{rev}$ of this type of material can attain 810 mAh/g at 0.1 C, while the C$_{irr}$ was 710 mAh/g. The capacity continues to fall off to 404 mAh/g after 20 cycles. Possible causes of the high C$_{irr}$ are detachment of the nanoparticles from the CNTs and the formation of the SEI layer over the CNTs. In a material like this, the SEI layer can isolate the more conductive CNTs and drive up the loss.

A material that may have effectively maintained good contact between the CNTs after the SEI was formed consisted of CNT sheets of aligned tubes.[26] The CNT sheets were also coated with SnO$_2$ nanoparticles (Figure 5). The sheets were functionalized with poly(vinylpyrrolidone), which captured the SnO$_2$ nanoparticles. This resulted in an anode material with very stable performance, up to 950 mAh/g (C$_{rev}$) at 0.1C over 70 cycles. Another aid to the high reversible capacity was that the material was tested as single sheets, eliminating the additional loss of conductivity that occurs as anode materials become thicker. As we saw in graphene anodes, the best performance is obtained when the anode thickness is minimized.

Depositing uniform tin coatings onto CNTs avoids the complications caused by the expansion of tin as it alloys with lithium. Also, placing the tin in direct contact with the CNTs allows the CNTs to be used as current carriers. Despite the promising results, tin's capacity is greatly exceeded by silicon's and there is far more to be gained by creating a Si/C nanocomposite.
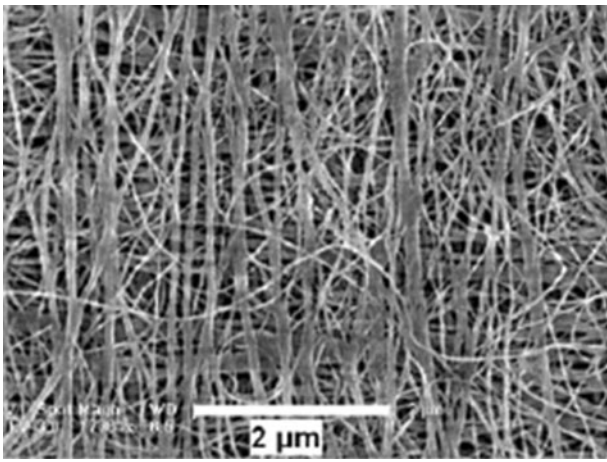
Fig. 5—SEM image of aligned and SiO_2 coated CNTs for a Li-ion battery anode.[26]

V. INTERCALATION AND ALLOYING

Understanding lithium intercalation is essential regardless of the anode material being considered. However, due to the obvious differences in structure between SWNTs, MWNTs, and metals, lithium uptake will take place in different ways.

Depending on the fabrication method and additional processing, CNTs may be open or close ended. The interior of closed CNTs is not accessible to lithium. Therefore, another mechanism is necessary for intercalation. Matsumura et al.[52] proposed that lithium is intercalated between graphene sheets, doped at graphene layer edges, and doped onto the surface of layers. If the CNT caps are removed, some believe that lithium may be intercalated in the interior of the tubes.[8,14] However, it is also suspected that lithium intercalated into the interior of tubes cannot be removed and contributes to the irreversible capacity.

Most of the loss of reversible capacity in carbon anodes takes place after the first lithiation, and part of this irreversible capacity is attributed to the formation of the SEI[53–55] on the surface of the anode. Additional processing of the CNTs, such as ball milling, increases capacity by fracturing the tubes and creating defects for lithium intercalation. Again, the lithium is not easily deintercalated from these defect sites, and the irreversible capacity is much higher than in raw CNTs.

In the case of nanowires, lithium alloys into the sides and causes a noticeable change in the nanowire profile (Figure 1), expanding its volume by 400 pct for silicon, 370 pct for germanium, and 300 pct for tin-oxide.[23,28] As discussed previously, in nanowires, the SEI is not the only cause of capacity loss and breakage of the nanowires is suspected.

Silicon atoms can alloy with a maximum of 4.4 lithium atoms, yielding a $Li_{22}Si_5$ alloy when its theoretical specific capacity of 4200 mAh/g is attained.[28,56,57] At this point, the Li-Si unit cell is at its maximum volume (659.2 $Å^3$). As the lithium dealloys, the volume quickly drops. Since the original volume of the silicon atom is 160 $Å^3$,[28] it is very difficult for the lithiated

silicon atoms to maintain contact with a surrounding matrix as it shrinks. Therefore, as the electrical contact becomes less robust, less lithium can be removed from the anode. Even germanium and tin-oxide, with lower levels of expansion as they alloy with lithium than silicon, are faced with an identical problem. Germanium forms a $Li_{22}Ge_5$ alloy when saturated with lithium and has a theoretical capacity of 1625 mAh/g.[25]

The alloying process for tin-oxide was proposed to be more complex.[58] It is a two-stage process where lithium first binds to the oxygen atoms to form $2Li_2$. This reaction is not reversible. The tin reacts with lithium to form Li_xSn, which in its fully lithiated form is a $Li_{4.4}Sn$ alloy with a theoretical capacity of 994 mAh/g.[59]

To compensate for irreversible losses, Li-ion cells are normally made with excess cathode material, and this increases the overall cost of the battery.[60] For this and other reasons, improvements to the anode must be matched by improvements to the cathode to more completely address performance issues in the batteries.

VI. DISCUSSION

In this review, we see that while several options exist for developing improved lithium-ion battery anodes, none are without their drawbacks due to specific failure mechanisms. Nevertheless, each material shows the capability to exceed the performance of graphite.

In carbon nanotube based anodes, the losses may be a result of the greater surface area of the CNTs, and it was observed that the irreversible capacity frequently increases linearly with the surface area.[61] However, it has also been shown that a low irreversible capacity is not so much proportional to the Brunauer, Emmett, and Teller specific surface area of the carbon, but to the active surface area (ASA).[62] Each of these assertions are correct but apply to specific conditions. The former is more applicable to raw CNTs and graphite, while the latter applies more to modified carbons such as ball-milled or acid etched CNTs. Ball milling or acid etching the CNT exposes more of the basal plane edges of the graphene layers and increases the ASA. Each of these mechanisms drives greater formation of SEI, which in turn allows more Li^+ to be trapped. It should be noted, though, that the ASA can be reduced by coating the material with hard carbon or pyrolytic carbon.[62]

While silicon nanowires theoretically should provide high reversible capacity with very little losses, this is often not the case. Because of the one-dimensional geometry of the nanowires, they are very resistant to pulverization. However, since the current collectors to which the nanowires are attached do not expand with the nanowires, there is likely a stress buildup at the base of them. This can cause the nanowires to break free from the current collectors. Two-phase nanowires were conceived to provide a more secure attachment to the current collector and reduce losses due to nanowire breakage.[36] According to the high efficiency reported on these nanowires, this may seem to be the case. On the other hand, the high efficiency occurs from the second cycle onward and there is still a considerable first cycle

loss. If there is indeed no breakage of the nanowires, this loss may be attributed to the trapping of Li^+ within the silicon matrix.

Tin-oxide and germanium nanowires are subject to the same benefits and failure mechanisms as the silicon nanowires. It may also be possible to fabricate two-phase SnO_2 and germanium nanowires. However, these nanowires may also have a limit on the cutoff voltage that can be used. Single-phase SnO_2 nanowires were capable of a 24 pct efficiency over 50 cycles.[38] Most of the loss occurred on the first cycle where the efficiency was 29 pct. This could be an indication of nanowire breakage as well as Li^+ being trapped within the material.

Given the limitations on using nanosized carbons or silicon independently to boost the capacity, some research teams have decided that the most viable way to go seems to be with nanocomposites. Carbon or CNTs can form the structure of an anode and simultaneously function as pathways for the current. This will yield a material with a capacity somewhere between that of carbon and the metal infused into its matrix. Nonetheless, nanocomposites come with their own share of issues.

The primary failure mechanism in silicon nanocomposites is the separation between the silicon nanoparticles and the rest of the matrix that develops as the anode is cycled. As we know, the silicon nanoparticles expand when they alloy with lithium. This expansion pushes away neighboring components of the anode. However, as the silicon nanoparticles dealloy with the lithium and shrink, a gap is created (Figure 2). The nanoparticles may remain in contact with a portion of the anode matrix, but it is equally likely that if the anode is infused with electrolyte, the nanoparticles may float out of contact with the anode matrix and become isolated. In these nanocomposites, it is necessary to put a mechanism in place to firmly connect the silicon nanoparticles to a part of the matrix and ensure that they do not lose electrical contact when delithiating.

Carbon-coated silicon anodes are subject to a similar failure mechanism. In this case, as the silicon expands, it causes the carbon coating to expand. However, as the silicon contracts, the carbon coating does not contract with it. The silicon may then remain in partial contact with the rest of the anode matrix or become isolated if it is suspended in the electrolyte.

In the SnO_2 nanocomposites discussed in this article, the preceding failure mechanism is applicable, but with a key difference. In nanocomposites where tin-oxide is attached to CNTs through a functionalization mechanism, it is likely that the capacity loss occurs when SnO_2 nanoparticles break free of the CNTs. While the claim was made that the coating was smooth, distinct SnO_2 orbs are visible in the transmission electron micrograph in Figure 4. These orbs may exert stresses upon each other as they expand, causing some portion to be broken from contact with the CNT.

As seen in the SnO_2 coated aligned CNTs and the graphene sheets, the best performance may be obtained when thin materials, on the order of a few nanometers thick, are used. If thicker materials are used, we can expect that the irreversible losses will increase unless a mechanism is put in place to ensure electrical connectivity is retained between the layers. Another contributor to the performance of the SnO_2 coated sheets may be the method of binding the SnO_2 nanoparticles to the CNTs. This functionalization method may simply be very robust.

Despite the promising results presented here, there may still be a logical limit to the capacity an anode should have. In fact, one can argue there is as much, possibly more, to be gained by focusing on increasing the cathode capacity. Increasing the anode capacity from 372 to 1200 mAh/g (with a 140 mAh/g cathode capacity) can yield a 19 pct reduction in battery size. However, increasing the cathode capacity from 140 to 200 mAh/g (with a 372 mAh/g anode capacity) can lead to a 22 pct reduction in battery size. Therefore, should more attention be paid to increasing the cathode performance? A strong case can be made for this.

VII. CONCLUSIONS

Several avenues are available for improving lithium-ion battery performance *via* higher capacity anodes. SWNT anodes have experimentally yielded reversible capacities of up to 1000 mAh/g. MWNT anodes have attained 681 mAh/g. Unfortunately, CNTs are quite expensive, and for these anodes to be commercially viable, the cost must come down. However, CNT production is becoming more efficient and this will eventually lower the cost. Silicon and tin are inhibited by their tendency to expand when alloyed with lithium, but this can be overcome when they are formed into nanocomposites or nanowires. Ultimately, no perfect anode material may exist, but there are several opportunities to develop a material that balances good capacity, durability, and affordability.

REFERENCES

1. B. Gao, C. Bower, J.D. Lorentzen, L. Fleming, A. Kleinhammes, X.P. Tang, L.E. McNeil, Y. Wu, and O. Zhou: *Chem. Phys. Lett.*, 2000, vol. 327, pp. 69–75.
2. A.P. Legrand and S. Flandrois: *Chemical Physics of Intercalation Compounds,* Plenum, New York, NY, 1987, vol. 59.
3. H. Zhao, J. Rena, X. Hea, J Li, C. Jiang, and C. Wan: *Electrochim. Acta*, 2007, vol. 52, pp. 6006–11.
4. J. Shim and K.A. Striebel: *The Dependence of Natural Graphite Anode Performance on Electrode Density*, Lawrence Berkeley National Laboratory, Berkeley, CA, 2003.
5. M. Letellier, F. Chevallier, and M. Morcette: *Carbon*, 2007, vol. 45, pp. 1025–34.
6. H. Huang, W.K. Zhang, and X.P. Gan: *Mater. Chem. Phys.*, 2007, vol. 104, pp. 271–75.
7. Z. Yang and H. Wu: *Solid State Ionics*, 2001, vol. 143, pp. 173–80.
8. B. Gao, A. Kleinhammes, X.P. Tang, C. Bower, L. Fleming, Y. Wu, and O. Zhou: *Chem. Phys. Lett.*, 1999, vol. 307, pp. 153–57.
9. C. Bower, S. Suzuki, K. Tanigaki, and O. Zhou: *Appl. Phys.*, 1998, vol. A67, pp. 47–52.
10. D. Guyomard and J.M. Tarascon: *J. Electrochem. Soc.*, 1992, vol. 139, pp. 937–48.
11. J.Y. Eom, H.S. Kwon, J. Liu, and O. Zhou: *Carbon*, 2004, vol. 42, pp. 2589–96.

12. M.S. Dresselhaus, G. Dresselhaus, and P. Avouris: *Carbon Nanotubes: Synthesis Structure Properties, and Application*, Springer, New York, NY, 2001, pp. 391–425.
13. C. Journet and P. Bernier: *Appl. Phys.*, 1998, vol. A67, pp. 1–9.
14. G. Maurin, C. Bousquet, F. Henn, P. Bernier, R. Almairac, and B. Simon: *Chem. Phys. Lett.*, 1999, vol. 312, pp. 14–18.
15. F. Disma, L. Aymard, L. Dupont, and J.M. Tarascon: *J. Electrochem. Soc.*, 1996, vol. 143, pp. 3959–72.
16. B.J. Landi, M.J. Ganter, C.M. Schauerman, C.D. Cress, and R.P. Raffaelle: *J. Phys. Chem.*, 2008, vol. 122, pp. 7509–15.
17. S.H. Ng, J. Wang, Z.P. Guo, J. Chen, G.X. Wang, and H.K. Liu: *Electrochem. Acta*, 2005, vol. 51, pp. 23–28.
18. F. Flandrois and B. Simon: *Carbon*, 1999, vol. 37, pp. 165–80.
19. Y.P. Wu, E. Rahm, and R. Holze: *J. Power Sources*, 2003, vol. 114, pp. 228–36.
20. B.J. Landi, R.A. DiLeo, C.M. Schauerman, C.D. Cress, M.J. Ganter, and R.P. Raffaelle: *J. Nanosci. Nanotechnol.*, 2008, vol. 8, pp. 1–5.
21. P. Lian, X. Zhu, S. Liang, Z. Li, W. Yang, and H. Wang: *Electrochim. Acta*, 2010, vol. 55, pp. 3909–14.
22. E. Yoo, J. Kim, E. Hosono, H. Zhou, T. Kudo, and I. Honma: *Nano Lett.*, 2008, vol. 8, pp. 2277–82.
23. C.K. Chan, H. Peng, G. Liu, K. McIlwrath, X.F. Zhang, R.A. Huggins, and Y. Cui: *Nat. Nanotechnol.*, 2008, vol. 3, pp. 31–35.
24. C.K. Chan, X.F. Zhang, and Y. Cui: *Nano Lett.*, 2007, web published 12/21/2007.
25. L. Baggetto and P.H.L. Notten: *J. Electrochem. Soc.*, 2009, vol. 156, pp. A169–A175.
26. H.X. Zhang, C. Feng, Y.C. Zhai, K.L. Jiang, Q.Q. Li, and S.S. Fan: *Adv. Mater.*, 2009, vol. 21, pp. 2299–304.
27. R.A. Huggins: *J. Power Sources*, 1999, vol. 81, pp. 13–19.
28. B.A. Boukamp, G.C. Lesh, and R.A. Huggins: *J. Electrochem. Soc.*, 1981, vol. 128, pp. 725–29.
29. U. Kasavajjula, C. Wang, and A.J. Appleby: *J. Power Sources*, 2007, vol. 163, pp. 1003–39.
30. J. Yang, M. Winter, and J.O. Besenhard: *Solid State Ionics*, 1996, vol. 90, pp. 281–87.
31. R.A. Huggins and W.D. Nix: *Ionics*, 2000, vol. 6, pp. 57–63.
32. K. Lew, L. Pan, E. Dickey, and J. Redwing: *Adv. Mater.*, 2003, vol. 24, pp. 2073–76.
33. M. Huang, Y. Wu, H. Feick, N. Tran, E. Weber, and P. Yang: *Adv. Mater.*, 2001, vol. 13 (2), pp. 113–16.
34. A. Golovin, S. Davis, and P. Voorhees: *J. Appl. Phys.*, 2008, vol. 104, pp. 074301–11.
35. S. Roper, S. Davis, S. Norris, and A. Golovin: *J. Appl. Phys.*, 2007, vol. 102, pp. 034304–10.
36. L.F. Cui, R. Ruffo, C.K. Chan, H. Peng, and Y. Cui: *Nano Lett.*, 2009, vol. 9 (1), pp. 491–95.
37. A.M. Morales and C.M. Lieber: *Science*, 1998, vol. 279, pp. 208–11.
38. Y.D. Ko, J.G. Kang, J.G. Park, S. Lee, and D.W. Kim: *Nanotechnology*, 2009, vol. 20, pp. 455701–06.
39. M.K. Datta and P.N. Kumta: *J. Power Sources*, 2007, vol. 165, pp. 368–78.
40. I.S. Kim and P.N. Kumta: *J. Power Sources*, 2004, vol. 136, pp. 145–49.
41. K.J. Gross, J.C.F. Wang, and G.A. Roberts: U.S. Patent Application Publication US2004/137327 A1, 2004.
42. G.X. Wang, J. Yao, and H.K. Liu: *Electrochem. Solid State Lett.*, 2004, vol. 7, pp. A250–53.
43. C.S. Wang, G.T. Wu, X.B. Zhang, Z.F. Qi, and W.Z. Li: *J. Electrochem. Soc.*, 1998, vol. 145, pp. 2751–58.
44. M. Sherif El-Eskandarany, K. Sumiyama, and K. Suzuki: *J. Mater. Res. Soc.*, 1995, vol. 10, pp. 659–67.
45. X.Y. Yang, Z.W. Huang, Y.K. Wu, and H.Q. Ye: *Mater. Sci. Eng., A*, 2001, vol. A300, pp. 278–83.
46. M.K. Datta and P.N. Kumta: *J. Power Sources*, 2006, vol. 158, pp. 557–63.
47. Z. Luo, D. Fan, X. Liu, H. Mao, C. Yao, and Z. Deng: *J. Power Sources*, 2009, vol. 189, pp. 16–21.
48. Y.S. Jung, K.T. Lee, and S.M. Oh: *Electrochim. Acta*, 2007, vol. 52, pp. 7061–67.
49. Z. Wang, G. Chen, and D. Xia: *J. Power Sources*, 2008, vol. 184, pp. 432–36.
50. L. Shi, H. Li, Z. Wang, X. Huang, and L. Chen: *J. Mater. Chem.*, 2001, vol. 11, pp. 1502–05.
51. H. Li, X.J. Huang, L.Q. Chen, G.W. Zhou, Z. Zhang, and D.P. Yu: *Solid State Ionics*, 2000, vol. 181, pp. 135–37.
52. Y. Matsumura, S. Wang, and J. Mondori: *Carbon*, 1995, vol. 33, pp. 1457–62.
53. E. Peled: *J. Electrochem. Soc.*, 1979, vol. 126, pp. 2047–51.
54. M. Winter, J.O. Besenhard, M.E. Spahr, and P. Novak: *Adv. Mater.*, 1998, vol. 10, pp. 725–63.
55. H. Buqa, A. Wursig, J. Vetter, M.E. Spahr, F. Krumeich, and P. Novak: *J. Power Sources*, 2006, vol. 153, pp. 385–90.
56. R.R. Sharma and R.N. Seefurth: *J. Electrochem. Soc.*, 1976, vol. 128, pp. 1763–68.
57. C.V.D Marel, G.J.B. Vinke, and W.V.D. Lugt: *Solid State Commun.*, 1985, vol. 54, pp. 917–17.
58. I.A. Courtney and J.R. Dahn: *J. Electrochem. Soc.*, 1997, vol. 144, pp. 2045–52.
59. Y.G. Guo, J.S. Hu, and L.J. Wan: *Adv. Mater.*, 2008, vol. 20, pp. 2878–87.
60. W. Xing and J.R. Dahm: *J. Electrochem. Soc.*, 1997, vol. 144, pp. 1195–201.
61. G.C. Chung, S.H. Jun, K.Y. Lee, and M.H. Kim: *J. Electrochem. Soc.*, 1999, vol. 146, pp. 1664–71.
62. F. Beguin, F. Chevallier, C. Vix-Guterl, S. Saadallah, V. Bertagna, J.N. Rouzaud, and E. Frankowiak: *Carbon*, 2005, vol. 43, pp. 2160–67.